Mineralogical Magazine, February 2015, Vol. 79(1), pp. 205–216

Geschieberite, $K_2(UO_2)(SO_4)_2(H_2O)_2$, a new uranyl sulfate mineral from Jáchymov

J. Plášil[1,*], J. Hloušek[2,†], A. V. Kasatkin[3], R. Škoda[4], M. Novák[4] and J. Čejka[5]

[1] Institute of Physics ASCR, v.v.i., Na Slovance 2, CZ−182 21, Prague 8, Czech Republic
[2] U Roháčových kasáren 24, CZ−100 00, Prague 10, Czech Republic
[3] Fersmann Mineralogical Museum of the Russian Academy of Sciences, Leninsky Prospekt 18-2, 119071 Moscow, Russia
[4] Department of Geological Sciences, Faculty of Science, Masaryk University, Kotlářská 2, 611 37 Brno, Czech Republic
[5] Department of Mineralogy and Petrology, National Museum, Cirkusová 1740, CZ−193 00, Prague 9, Czech Republic

[*Received 27 July 2014; Accepted 7 October 2014; Associate Editor: G. D. Gatta*]

ABSTRACT

The new mineral geschieberite (IMA2014-006), $K_2(UO_2)(SO_4)_2(H_2O)_2$, was found in the Svornost mine, Jáchymov, Czech Republic, where it occurs as a secondary alteration phase after uraninite in association with adolfpateraite and gypsum. Geschieberite forms crystalline aggregates of bright green colour (when thick) composed of multiply intergrown prismatic crystals elongated on [001] typically reaching 0.1−0.2 mm across; observable forms are {010} and {001}. Crystals are translucent to transparent with a vitreous lustre. The mineral is brittle, with perfect cleavage on {100} and an uneven fracture. It has a greenish-white streak and a probable Mohs hardness of ~2. The mineral is slightly soluble in cold H_2O. The calculated density is 3.259 g cm^{-3}. The mineral exhibits strong yellowish-green fluorescence under both shortwave and longwave UV radiation. Optically, geschieberite is biaxial (−), with $\beta = 1.596(2)$ and $\gamma = 1.634(4)$ (measured at 590 nm), with X = a. Electron-microprobe analyses provided Na_2O 0.23, K_2O 14.29, MgO 2.05, CaO 0.06, UO_3 49.51, SO_3 27.74, H_2O 6.36 (structure), total 100.24 wt.%, yielding the empirical formula $(K_{1.72}Mg_{0.29}Na_{0.04}Ca_{0.01})_{\Sigma 2.06}(U_{0.98}O_2)(S_{0.98}O_4)_2(H_2O)_2$ based on 12 O atoms per formula unit. The Raman spectrum is dominated by the symmetric stretching vibrations of UO_2^{2+}, SO_4^{2-} and weaker O−H stretching vibrations. Geschieberite is orthorhombic, $Pna2_1$, with a = 13.7778(3), b = 7.2709(4), c = 11.5488(2) Å, V = 1156.92(7) Å^3, Z = 4. The eight strongest powder X-ray diffraction lines are [d_{obs} in Å (hkl) I_{rel}]: 6.882 (200) 100, 5.622 (111) 53, 4.589 (211) 12, 4.428 (202) 16, 3.681 (311) 18, 3.403 (013) 12, 3.304 (401,$\bar{1}$13) 15 and 3.006 (122) 17. The structure, refined to R = 0.028 for 1882 $I > 3\sigma(I)$ reflections, contains $[(UO_2)(SO_4)_2(H_2O)]^{2-}$ sheets that are based on the protasite anion topology. Sheets are stacked perpendicular to **a**. Potassium atoms and one H_2O molecule are located between these sheets, providing an interlayer linkage. The remaining H_2O molecule is localized within the structural unit, at the free vertex of the uranyl pentagonal bipyramid; this vertex does not link to sulfate tetrahedra. The mineral is named for one of the most important ore veins in Jáchymov − the Geschieber vein.

Keywords: geschieberite, new mineral, uranyl sulfate, crystal structure, Raman spectroscopy, Jáchymov.

Introduction

Uranyl sulfates are common alteration products resulting from the weathering of uraninite or other U-containing minerals, as well as vein sulfides,

* E-mail: plasil@fzu.cz
† deceased, April 27, 2014
DOI: 10.1180/minmag.2015.079.1.16

such as pyrite, marcasite or chalcopyrite. Oxidative weathering of sulfide minerals leads to the formation of solutions with quite low pH and high activity of anions such as SO_4^{2-} (Jambor *et al.*, 2000). These acidic solutions are referred to as acid mine drainage (AMD) when they have an anthropogenic origin, as e.g. minerals formed in old mining galleries and workings (Plášil, 2014). They are responsible for leaching and transport of heavy elements on a large scale (Edwards *et al.*, 2000; Evangelou and Zhang, 1995). Until recently, very few uranyl sulfates were known to occur in Nature, e.g. minerals of the zippeite group (Frondel *et al.*, 1976) and uranopilite (Burns, 2001). However, during the last few years a large number of new uranyl sulfates has been discovered from Jáchymov, Czech Republic (Plášil *et al.*, 2011, 2012, 2014*a*), France (Plášil *et al.*, 2013*a*), Utah, USA (Kampf *et al.*, 2014; Plášil *et al.*, 2013*b*, 2014*b*) and the Northern Caucasus, Russia (Pekov *et al.*, 2014). Here, we describe geschieberite, a new uranyl sulfate mineral from Jáchymov, Czech Republic.

The name geschieberite, originates from the name of one of the most important ore veins in Jáchymov – the Geschieber vein, exploited by the Svornost and Josef mines, in the town of Jáchymov. The new mineral and name have been approved by the Commission on New Minerals, Nomenclature and Classification (CNMNC) of the International Mineralogical Association (IMA2014-006, Plášil *et al*., 2014*c*). The type specimen is deposited in the collections of the Fersman Mineralogical Museum of the Russian Academy of Sciences, Moscow, Russia, registration number 4537/1.

Occurrence

Geschieberite was found underground by one of the authors (JH) in material originating from the Geschieber vein on the 5th level of the Svornost mine in Jáchymov, Western Bohemia, Czech Republic. The new mineral is extremely rare at the site and occurred on a single specimen. It was found closely associated with gypsum, adolfpateraite (Plášil *et al.*, 2012), mathesiusite (Plášil *et al.*, 2014*a*) and a new mineral, svornostite, $K_2Mg[(UO_2)(SO_4)_2]_2{\cdot}8H_2O$) (Plášil *et al.*, 2015).

Physical and optical properties

Geschieberite occurs in a bright green, compact crystalline aggregates (Fig. 1). This crusty aggregate consists of multiple intergrowths of 0.1–0.2 mm long prismatic crystals. The only crystal faces observed belong to the prism forms {001} and {010}. Individual crystals are of paler green colour and have a vitreous lustre. Geschieberite has a greenish-white streak. The Mohs hardness could not be measured, but is probably ~2. The mineral is brittle with an uneven fracture. There is one perfect cleavage on {100}. The mineral is slightly soluble in cold H_2O. The density of 3.259 g cm^{-3} was calculated using the empirical formula and unit-cell parameters obtained from single-crystal X-ray diffraction (XRD) data. Density measurements could not be performed due to the extreme paucity of pure material. Geschieberite exhibits strong fluorescence (yellowish green) under both shortwave and longwave UV radiation.

In thin fragments in plane-polarized transmitted light, geschieberite is nearly colourless and exhibits no apparent pleochroism. Optically, geschieberite is biaxial (–), with β = 1.596(2) and γ = 1.634(4) (measured at 590 nm) and a partially determined optical orientation is X = a. These two indices of refraction were measured on thin {100} cleavage fragments. Due to incomplete optical data the Gladstone-Dale compatibility index (Mandarino, 1981) could not be calculated. The n_{mean} value calculated from the Gladstone-Dale compatibility index is 1.53 (for ideal compatibility).

Chemical composition

The chemical composition of geschieberite (Table 1) was determined using a Cameca SX100 electron microprobe (wavelength

FIG. 1. Massive crystal aggregate of geschieberite (light green), with gypsum (whitish). Field of view is 3.0 mm (photo P. Škácha).

https://doi.org/10.1180/minmag.2015.079.1.16 Published online by Cambridge University Press

TABLE 1. Results of WDS analyses (wt.%) of geschieberite.

	Mean (n = 7)	Range	SD
Na_2O	0.23	0.12–0.59	0.17
K_2O	14.29	12.90–16.66	1.27
MgO	2.05	1.77–2.52	0.29
CaO	0.06	bdl–0.12	0.04
SO_3	27.74	26.82–28.78	0.74
UO_3	49.51	47.23–51.64	1.43
H_2O*	6.36		
Total	101.16		

bdl: below detection limit
* Calculated

dispersive spectroscopy (WDS) mode, 15 kV, 4 nA, 15 μm beam diameter) from seven point analyses. The following X-ray lines and standards were used: $K\alpha$ lines: S ($SrSO_4$), Ca (fluorapatite), Mg (Mg_2SiO_4), K (sanidine), Na (albite); $M\beta$ lines: U (uranophane). Peak counting times were 10–20 s and the counting time for background was 50% of that of the peak. Measured intensities were processed for matrix effects using the '*PAP*' correction routine (Pouchou and Pichoir, 1985).

Analytical results are given in Table 1. The empirical formula of geschieberite, based on these results, calculated by stoichiometry obtained from the crystal structure (12 O atoms per formula unit) is $(K_{1.72}Mg_{0.29}Na_{0.04}Ca_{0.01})_{\Sigma 2.06}(U_{0.98}O_2)(S_{0.98}O_4)_2(H_2O)_2$. The ideal formula is $K_2(UO_2)(SO_4)_2(H_2O)_2$, which requires K_2O 16.38, UO_3 49.56, SO_3 27.80 and H_2O 6.26, total 100.00 wt.%.

Raman spectroscopy

The Raman spectrum of geschieberite (Fig. 2) was collected on a Thermo Scientific DXR Raman Microscope interfaced with an Olympus microscope (objective 50×) in the 50–3500 cm^{-1} range with ~2 cm^{-1} resolution. The power of the frequency-stabilized single-mode diode laser (532 nm) impinging on the sample was limited to 3 mW (60 s exposure, accumulation of 20 scans). The spectrophotometer was calibrated by a software-controlled (*Omnic 8*) calibration procedure using multiple neon emission lines (wavelength calibration), multiple polystyrene

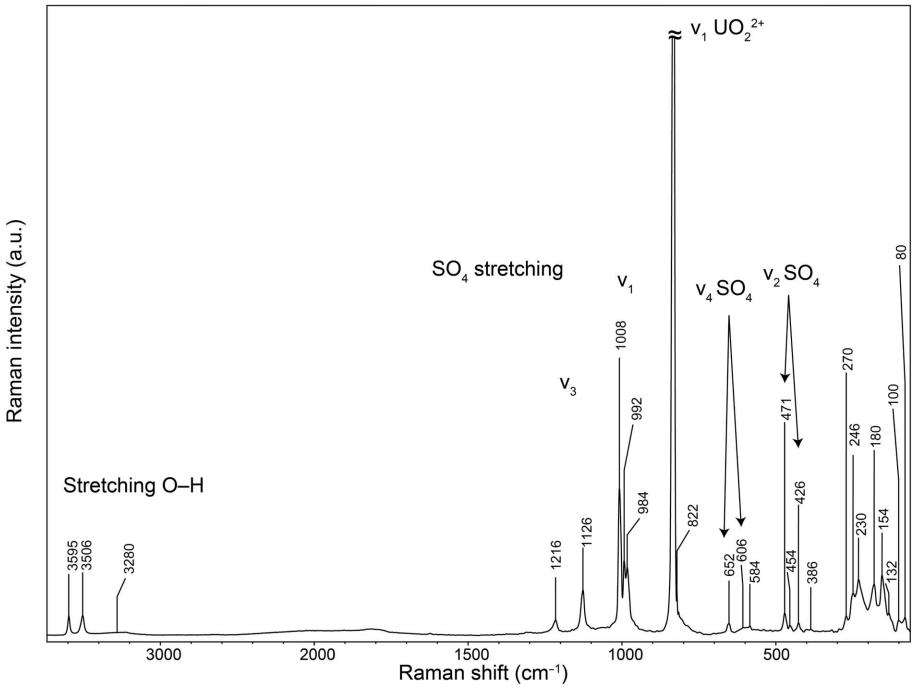

FIG. 2. Raman spectrum of geschieberite with assigned vibration regions.

https://doi.org/10.1180/minmag.2015.079.1.16 Published online by Cambridge University Press

Raman bands (laser frequency calibration) and standardized white-light sources (intensity calibration). Spectroscopic manipulation, background correction and band component analysis, was undertaken with *Omnic 8* software. The interpretation of the spectrum followed the papers of Nakamoto (1986), Čejka (1999, 2004, 2007), Niinistö *et al.* (1978) and Plášil *et al.* (2010, 2012). For general comparison, the infrared spectrum of synthetic $(NH_4)_2UO_2(SO_4)_2{\cdot}2H_2O$ (Niinistö *et al.*, 1978) contains the following absorption bands (in cm^{-1}): 3600 and 3500 (ν H_2O), 3175 (ν_3 NH_4^+), 3000sh (ν_1 NH_4^+), 2850 ($2\nu_4$ NH_4^+), 1990 (ν_1 SO_4), 1620 and 1595 (δ H_2O), 1425 (ν_4 NH_4^+), 1205, 1165sh, 1120, 1060, 1020sh (ν_3 SO_4^{2-}), 990 (ν_1 SO_4^{2-}), 924 (ν_3 UO_2^{2+}), 836 (ν_1 UO_2^{2+}), 640, 910, 590sh, 580 (ν_4 SO_4^{2-}) and 470, 455, 435, 425 (ν_2 SO_4^{2-}).

In the structure of geschieberite, there are one symmetrically unique U^{6+} (in the form of uranyl, UO_2^{2+}), two symmetrically distinct S^{6+} (in the form of the sulfate anion, SO_4^{2-}), two symmetrically distinct K^+ and two structurally non-equivalent water molecules.

A band at 832 cm^{-1}, with the highest observed intensity, is attributed to the ν_1 $(UO_2)^{2+}$ symmetric stretching vibration. According to the relation given by Bartlett and Cooney (1989), the approximate U–O bond length is 1.78 Å. A shoulder at 822 cm^{-1} may also be related to the ν_1 $(UO_2)^{2+}$ symmetric stretching vibration (with corresponding U–O bond length of ~1.79 Å) or libration of H_2O. For comparison, corresponding U–O bond lengths in geschieberite obtained from the X-ray data are 1.781(4) and 1.786(4) Å (see structure description below). For the synthetic analogue studied by Alekseev *et al.* (2006), the U–O lengths are 1.760(3) and 1.763(3). No band related to the ν_3 $(UO_2)^{2+}$ antisymmetric stretching vibration was observed. This is in accordance with the rule that this vibration is generally active in infrared and not in Raman. The bands at 270, 250 and 230 cm^{-1} are then attributed to the doubly degenerate ν_2 (δ) $(UO_2)^{2+}$ modes.

Bands of medium intensity located at 1216, 1126 and 1008 cm^{-1}, as well as those at 992 and 984 cm^{-1}, were assigned to the split triply degenerate ν_3 $(SO_4)^{2-}$ antisymmetric stretching vibration and the ν_1 $(SO_4)^{2-}$ symmetric stretching vibration, respectively. Bands at 652, 606 and 584 cm^{-1}, and at 470, 456 and 426 cm^{-1} are assigned to triply degenerate ν_4 (δ) $(SO_4)^{2-}$ bending vibrations and doubly degenerate ν_2 (δ) $(SO_4)^{2-}$ bending vibrations, respectively.

Raman bands with largest stretching energies, at 3594 and 3506 cm^{-1} (with a weak shoulder at 3280 cm^{-1}) are attributed to ν O–H stretching vibrations of the hydrogen-bonded H_2O molecules. According to the empirical relation provided by Libowitzky (1999), the corresponding approximate O–H···O hydrogen-bond lengths lie within the range of ~3.2 and 2.9 Å, respectively. For the synthetic compound, based on single-crystal XRD data, Alekseev *et al.* (2006) inferred hydrogen bonds with lengths of 2.697(5) and 2.933(5) Å related to the H_2O molecule within the $[UO_2(SO_4)_2(H_2O)]$ layers, and of 2.96(1) Å related to the H_2O molecule in the interlayer. Alekseev *et al.* (2006) described hydrogen bonds between terminal oxygen atoms of SO_4 groups and H_2O, located within the layer, and between H_2O located in the interlayer and H_2O from the layer (see below). A band at 1816 cm^{-1} is probably related to an overtone or is a combination band. No band related to the ν_2 (δ) H_2O bending vibration was observed in the Raman spectrum, which is not surprising due to the strong fluorescence of the material and, generally, poor sensitivity of Raman for bending H–O–H vibrations.

The Raman band observed at 386 cm^{-1} may correspond to a libration mode of H_2O or ν $U–O_{equatorial}$. Very weak bands at ~350 cm^{-1} may be related to the K–O stretching vibrations (similar to K–O stretching vibrations in zippeite; Plášil *et al.*, 2010). The bands at the lowest energies are related to the lattice modes.

X-ray crystallography and structure determination

Powder XRD data for geschieberite (Table 2) were obtained from a hand-picked sample using a PANalytical Empyrean diffractometer equipped with a PIXcel^{3D} detector, employing Cu*K*α radiation (45 kV, 40 mA). The Debye-Scherrer geometry provided by focusing mirror-optics was used in order to reduce preferred orientation effects. The data were collected over the range 3–80º2θ, with a step size of 0.01º and counting time of 2 s per step (with accumulation of 20 scans). The positions and intensities of diffractions were found and refined using a Pseudovoigt shape function with the *High-Score* program (PANalytical B.V., Almelo, Netherlands). Unit-cell parameters were refined using least-squares with the *Celref* program (Laugier and Bochu, 2004). The theoretical

https://doi.org/10.1180/minmag.2015.079.1.16 Published online by Cambridge University Press

TABLE 2. Powder XRD data for geschieberite from Jáchymov.

I_{rel}	d_{obs}	d_{calc}	I_{calc}	h	k	l	I_{rel}	d_{obs}	d_{calc}	I_{calc}	h	k	l
100	6.882	6.893	86	2	0	0	3	2.150	2.153	3	6	1	1
1	6.519	6.436	1	1	1	0	2	2.134	2.134	5	6	0	2
7	6.155	6.155	10	0	1	1	2	2.128	2.127	1	2	3	2
4	5.789	5.768	4	0	0	2	1	2.113	2.116	1	4	1	4
53	5.622	5.620	100	1	1	1	2	2.098	2.095	7	2	1	5
1	5.004	5.005	<1	2	1	0	4	2.054	2.054	6	5	2	2
12	4.589	4.591	26	2	1	1			2.052	5	0	3	3
16	4.428	4.423	36	2	0	2	3	2.031	2.028	8	3	2	4
1	4.255	4.295	<1	1	1	2	2	1.9860	1.9837	6	3	1	5
3	3.783	3.780	3	2	1	2	6	1.9679	1.9665	12	2	3	3
18	3.681	3.682	35	3	1	1	2	1.9558	1.9551	7	4	3	1
1	3.629	3.639	<1	0	2	0	1	1.9256	1.9225	3	0	0	6
9	3.517	3.519	16	1	2	0	3	1.8759	1.8757	6	7	1	1
6	3.447	3.446	6	4	0	0	2	1.8555	1.8539	5	4	1	5
12	3.403	3.400	20	0	1	3	2	1.8407	1.8411	2	6	2	2
1	3.342	3.358	<1	2	0	3	2	1.8044	1.8039	3	1	4	0
15	3.304	3.302	3	4	0	1	2	1.7641	1.7630	6	4	3	3
		3.301	27	1	1	3	1	1.7473	1.7479	5	5	2	4
4	3.113	3.115	7	4	1	0	1	1.7325	1.7352	3	0	4	2
14	3.079	3.078	24	0	2	2	5	1.7227	1.7232	1	8	0	0
3	3.049	3.049	7	2	1	3	2	1.7183	1.7193	3	5	1	5
17	3.006	3.004	27	1	2	2	2	1.7039	1.7041	4	7	1	3
9	2.958	2.958	20	4	0	2	2	1.6896	1.6917	1	3	4	0
9	2.889	2.884	19	0	0	4	1	1.6830	1.6871	6	1	2	6
2	2.853	2.853	6	3	2	0	1	1.6728	1.6718	5	0	3	5
3	2.810	2.810	8	2	2	2	3	1.6605	1.6594	2	8	1	1
5	2.739	2.733	8	3	1	3	6	1.6519	1.6510	5	6	3	1
3	2.665	2.660	7	2	0	4	2	1.6467	1.6504	1	2	2	6
1	2.598	2.596	<1	1	2	3	2	1.6244	1.6247	4	2	3	5
2	2.558	2.557	5	3	2	2	1	1.6111	1.6112	2	6	2	4
5	2.517	2.516	10	5	1	1	1	1.6067	1.6072	2	0	1	7
1	2.495	2.502	1	4	2	0	1	1.5960	1.5964	3	1	1	7
6	2.375	2.374	11	0	3	1	1	1.5581	1.5574	2	8	2	0
11	2.297	2.298	7	6	0	0	2	1.5304	1.5304	4	6	3	3
6	2.247	2.245	14	2	3	1	3	1.4859	1.4864	2	9	1	1
5	2.233	2.230	11	1	2	4	1	1.4366	1.4363	2	1	5	1
4	2.176	2.172	7	1	1	5							

pattern, used for indexing the experimental dataset, was calculated from the structure data using *PowderCell* (Kraus and Nolze, 1996). Unit-cell parameters of geschieberite refined from the powder diffraction data are a = 13.786(5), b = 7.278(3), c = 11.536(4) Å, V = 1157.4(7) Å^3.

A 0.188 mm × 0.109 mm × 0.093 mm crystal fragment was used for the collection of structure data on an Oxford Diffraction Gemini single-crystal diffractometer. Graphite-monochromatized Mo$K\alpha$ radiation (λ = 0.71073 Å) from a conventional sealed X-ray tube, collimated with a fibre optics Mo-Enhance collimator was detected with an Atlas CCD detector. Correction for background, Lorentz effect and polarization was applied to the data during reduction in the *Crysalis* package (Agilent Technologies 2014, Oxford, UK). A Gaussian correction for absorption was performed, combining the correction for crystal shape and the empirical correction utilizing *Jana2006* (Petříček *et al.*, 2014). The correction led to the internal R factor of the dataset = 0.0362. Crystallographic details, data collection and refinement parameters are given in Table 3.

The structure was solved independently of previous structure determinations (Niinistö *et al.*,

https://doi.org/10.1180/minmag.2015.079.1.16 Published online by Cambridge University Press

1979; Alekseev *et al.*, 2006) by the charge-flipping algorithm (Oszlányi and Sütő, 2004, 2008; Palatinus, 2013) implemented in the *Superflip* program (Palatinus and Chapuis, 2007). The model obtained from the structure solution was refined by the full-matrix least-squares algorithm of the *Jana2006* program (Petříček *et al.*, 2006, 2014) based on F^2. Systematic absences and the structure solution by *Superflip* (Palatinus and van der Lee, 2008) indicates the centrosymmetric space group *Pnam*. However, in accordance with the results by Alekseev *et al.* (2006), the structure refinement confirmed the non-centrosymmetric $Pna2_1$ space group. The refinement carried out in the centrosymmetric choice (*Pnam*) led to a significantly worse result (R = 10%) and was unstable; not all the O atoms could be refined in this setting. The possible solution in the acentric space group was investigated and inversion twinning was introduced into the refinement, giving the ratio of the racemate of 0.48(2) (Table 3). Nearly all atoms were found by the structure solution, but several O atoms of the SO_4 groups and H_2O molecules were located from difference Fourier maps. The U, S and K sites were refined with anisotropic displacement parameters, but the O atoms were refined using isotropic displacement parameters. We note that H atoms can, to some extent, be localized from the difference Fourier maps, but we are convinced that the refined H positions are not reliable and are related to some

TABLE 3. Summary of data-collection conditions and refinement parameters for geschieberite.

Structural formula	$K_2(UO_2)(SO_4)_2(H_2O)_2$
Unit-cell parameters	a = 13.7778(4) Å
	b = 7.2709(2) Å
	c = 11.5488(3) Å
V (Å^3)	1156.92(6)
Z	4
Space group	$Pna2_1$
$D_{calc.}$ (g cm^{-3})	3.296
Temperature	300(2) K
Wavelength (Å)	Mo$K\alpha$, 0.71075
Crystal dimensions (mm)	0.19 × 0.11 × 0.09
Limiting θ angles (º)	2.96–29.39
Limiting Miller indices	$-17 \leqslant h < 18$, $-9 \leqslant k \leqslant 9$, $-14 \leqslant l \leqslant 15$
No. of reflections	16,670
No. of unique reflections	2901
No. of observed reflections (criterion)	2402 [$I > 3\sigma(I)$]
Absorption correction (mm^{-1}), method	15.16, gaussian
T_{min}/T_{max}	0.149/0.423
Completeness to 28.50º, R_{int}	0.94, 0.0362
F_{000}	1032
Refinement by *Jana2006* on F^2	
Param. refined, constraints, restraints	95, 0, 1
R_1, wR_2 (obs)	0.0282, 0.0648
R_1, wR_2 (all)	0.0346, 0.0681
Gof (obs, all)	1.53, 1.46
Weighting scheme	$1/(\sigma^2(I) + 0.0004I^2)$
Absolute structure	1332 Friedel pairs
Flack parameter	0.48(2)
$\Delta\rho_{min}$, $\Delta\rho_{max}$ (e Å^{-3})	−1.64, 2.33
Twin matrix	$\begin{pmatrix} -1 & 0 & 0 \\ 0 & -1 & 0 \\ 0 & 0 & -1 \end{pmatrix}$

https://doi.org/10.1180/minmag.2015.079.1.16 Published online by Cambridge University Press

TABLE 4. Atom positions and displacement parameters (U_{eq}, U_{iso}, in Å^2) for the structure of geschieberite.

Atom	*x*/*a*	*y*/*b*	*z*/*c*	U_{eq}	U^{11}	U^{22}	U^{33}	U^{12}	U^{13}	U^{23}
U1	0.255076(13)	0.91435(3)	0.250413(15)	0.01299(7)	0.01811(13)	0.00904(12)	0.01181(12)	−0.00029(7)	−0.0012(5)	−0.0034(3)
K1	0.0698(5)	0.2399(5)	0.0351(2)	0.0324(17)	0.023(3)	0.020(2)	0.054(3)	−0.0006(18)	0.005(3)	−0.0049(18)
K2	−0.0710(5)	−0.2371(6)	−0.0383(2)	0.0311(17)	0.024(3)	0.022(2)	0.047(3)	0.0010(19)	−0.001(2)	−0.0041(19)
S1	0.1762(5)	0.7435(5)	−0.0313(3)	0.0144(15)	0.018(3)	0.012(2)	0.013(2)	0.0014(14)	0.000(2)	−0.0036(14)
S2	−0.1766(5)	−0.7442(5)	0.0283(3)	0.0157(16)	0.023(3)	0.008(2)	0.016(2)	−0.0016(14)	0.000(2)	0.0011(14)
O1	0.2352(3)	0.0687(6)	0.7543(15)	0.0240(12)*						
O2	0.2461(8)	0.797(2)	0.0624(9)	0.019(3)*						
O3	−0.2483(9)	−0.785(2)	−0.0652(9)	0.020(3)*						
O4	0.2584(7)	1.1703(18)	0.1244(8)	0.016(3)*						
O5	−0.2657(8)	−1.1720(18)	−0.1282(8)	0.020(3)*						
O6	0.0681(3)	0.3995(6)	0.2474(15)	0.0381(12)*						
O7	0.1059(9)	0.6094(17)	0.0020(7)	0.027(3)*						
O8	−0.1093(8)	−0.6058(15)	−0.0167(7)	0.021(2)*						
O9	0.1330(8)	0.9146(13)	−0.0712(8)	0.020(3)*						
O10	−0.1228(9)	−0.9086(13)	0.0655(8)	0.023(3)*						
O11	0.3832(3)	0.8966(5)	0.2555(10)	0.0198(10)*						
O12	0.1264(3)	0.9326(5)	0.2556(11)	0.0219(11)*						

* Refined isotropically.

artifact in the data – the difference electron density might arise from undescribed absorption effects or the contribution of the weak split-crystal domain, which is probably present. However, the refined twin fraction is unreliable, having a similar order to the experimental error from the refinement. Therefore we present here the structure model without H atoms. The final refinement for 105 parameters converged to R = 0.0282, wR = 0.0648 for 1882 observed reflections with Gof = 1.43. Atom coordinates and displacement parameters are listed in Table 4. The bond-valence analysis (after Brown, 1981, 2002), based on refined interatomic distances (Table 5) is provided in Table 6. The crystallographic information file (CIF) and the structure factors list have been deposited with the Principal Editor of *Mineralogical Magazine* and are available from www.minersoc.org/pages/e_journals/dep_mat_mm.html.

TABLE 5. Selected interatomic distances (in Å) for geschieberite.

U1–O1^{i}	2.517(4)	S1–O2	1.499(13)
U1–O2	2.337(11)	S1–O5^{iii}	1.471(11)
U1–O3^{ii}	2.331(12)	S1–O7	1.427(13)
U1–O4	2.362(12)	S1–O9	1.454(11)
U1–O5^{ii}	2.344(12)	<*S1–O*>	1.463
U1–O11	1.770(4)		
U1–O12	1.779(4)	S2–O3	1.493(12)
<*U–O$_{Ur}$*>	1.775	S2–O4^{vi}	1.524(11)
<*U–O$_{eq}$*>	2.378	S2–O8	1.463(12)
		S2–O10	1.470(11)
		<*S2–O*>	1.488
K1–O3^{iii}	2.780(13)	K2–O2^{vi}	2.810(13)
K1–O4^{iv}	2.841(12)	K2–O5^{v}	2.915(13)
K1–O6	2.712(16)	K2–O6^{vii}	2.742(16)
K1–O7	2.759(13)	K2–O7^{iv}	2.721(14)
K1–O8^{v}	2.777(13)	K2–O8	2.744(12)
K1–O9^{iv}	2.804(10)	K2–O10^{v}	2.767(10)
K1–O10^{v}	2.887(14)	<*K2–O*>	2.78
<*K1–O*>	2.79		
O1–O2^{viii}	2.779(19)	O3–O11^{vii}	2.899(15)
O1–O3^{ix}	2.619(19)	O3–O12^{vii}	2.875(15)
O1–O6^{viii}	2.977(6)	O4–O5^{ii}	2.858(13)
O1–O9^{x}	2.701(16)	O4–O8^{xii}	2.489(14)
O1–O10$^{xi,\ H}$	2.917(16)	O4–O10^{xii}	2.479(16)
O1–O11$^{viii,\ H}$	2.888(5)	O4–O12	2.931(13)
O2–O4	2.82(2)	O5–O7^{xiii}	2.366(15)
O2–O5^{iii}	2.386(15)	O5–O9^{xiii}	2.343(16)
O2–O7	2.463(18)	O5–O11^{vii}	2.903(13)
O2–O9	2.355(16)	O5–O12^{vii}	2.918(13)
O2–O12	2.945(15)	O6–O11$^{xiv,\ H}$	2.950(6)
O3–O4^{vi}	2.344(15)	O6–O12$^{x,\ H}$	3.490(6)
O3–O5	2.92(2)	O7–O9	2.403(15)
O3–O8	2.380(17)	O8–O10	2.405(14)
O3–O10	2.466(16)		

Symmetry codes: (i) $-x+1/2$, $y+1/2$, $z-1/2$; (ii) $-x$, $-y$, $z+1/2$; (iii) $x+1/2$, $-y-1/2$, z; (iv) x, $y-1$, z; (v) x, $y+1$, z; (vi) $x-1/2$, $-y+1/2$, z; (vii) $-x$, $-y$, $z-1/2$; (viii) $-x+1/2$, $y-1/2$, $z+1/2$; (ix) $x+1/2$, $-y-1/2$, $z+1$; (x) x, $y-1$, $z+1$; (xi) $-x$, $-y-1$, $z+1/2$; (xii) $x+1/2$, $-y+1/2$, z; (xiii) $x-1/2$, $-y-1/2$, z; (xiv) $x-1/2$, $-y+3/2$, z.
H – most probably corresponding to the H bonds.

https://doi.org/10.1180/minmag.2015.079.1.16 Published online by Cambridge University Press

TABLE 6. Bond-valence analysis for geschieberite.

	U	S1	S2	K1	K2	ΣBV	Assignment	H^+
O1	0.40					0.40	H_2O	2×0.8
O2	0.56	1.40			0.16	2.12	O	
O3	0.57		1.42	0.17		2.16	O	
O4	0.54		1.31	0.15		2.00	O	
O5	0.56	1.51			0.12	2.19	O	
O6				0.21	0.19	0.40	H_2O	2×0.8
O7		1.70		0.18	0.20	2.08	O	
O8			1.55	0.17	0.19	1.91	O	
O9		1.58		0.16	0.18	1.92	O*	
O10			1.52	0.13		1.65	O*	$+2 \times 0.2$
O11	1.72					1.72	O*	$+0.2^{\#}$
O12	1.69					1.69	O*	$+2 \times 0.2$
ΣBV	6.04	6.19	5.80	1.17	1.04			

Values are given in valence units (vu). ΣBV = sum of bond valences incident at the atomic site. H^+ – contribution by corresponding H bonds (in vu). U^{6+}–O bond-valence parameters (r_0 = 2.045, b = 0.51) taken from Burns *et al.* (1997); K^+–O and S^{6+}–O bond-valence parameters taken from Brown and Altermatt (1985).* Anions act as acceptors of the bond valence by H bond contribution. #Corresponds to the weak H bond between O6 and O12 (2.6 Å ~ 0.12 vu).

Description of the crystal structure

The structure of geschieberite (Fig. 3*a*) contains one U, two S, two K, 12 O and four H atom sites in the asymmetric unit. The structure of geschieberite is the same as that reported for the synthetic compound $K_2[(UO_2)(SO_4)_2(H_2O)](H_2O)$ by Niinistö *et al.* (1979) and Alekseev *et al.* (2006). The *U* site is occupied by U^{6+} (Table 4), coordinated by seven ligands forming a squat pentagonal bipyramid, with observed bond distances typical for [7]-coordinate U^{6+} (Burns *et al.*, 1997). The *S* site is [4]-coordinated by O atoms forming a quite regular tetrahedron. Uranyl pentagonal bipyramids, water molecules and sulfate tetrahedra link to form a uranyl sulfate sheet of composition $[(UO_2)(SO_4)_2(H_2O)]^{2-}$. These sheets are based on the protasite anion topology (Burns, 2005) in which uranyl pentagonal bipyramids are connected by sharing vertices with sulfate

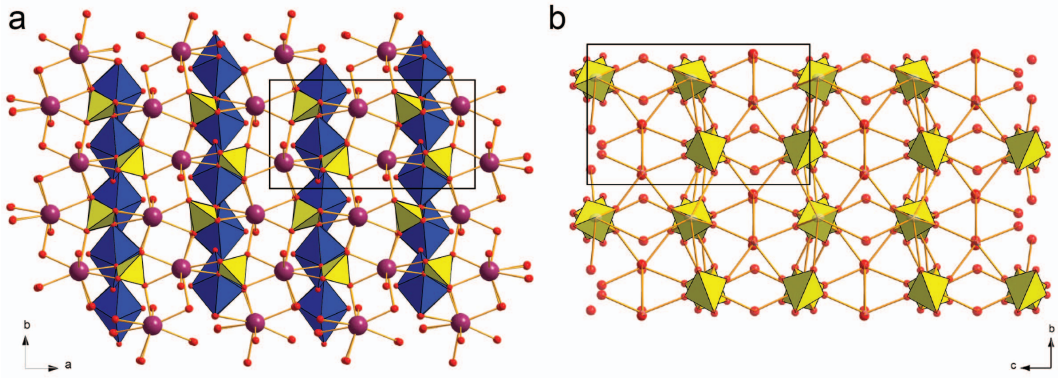

FIG. 3. (*a*) Crystal structure of geschieberite viewed along **c**. Uranyl sulfate sheets are stacked perpendicular to **a**, and between them, K^+ cations and a H_2O group are localized, providing a link between adjacent sheets. UO_7 bipyramids are blue, SO_4 are yellow, K atoms are violet, O atoms are red. Unit-cell edges are outlined by a solid black line. (*b*) Overlap of the misoriented SO_4 groups viewed along **a**.

https://doi.org/10.1180/minmag.2015.079.1.16 Published online by Cambridge University Press

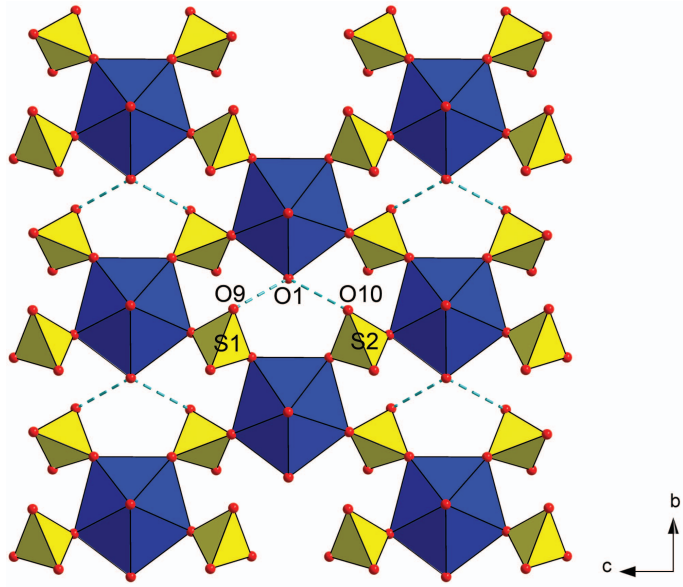

FIG. 4. The uranyl sulfate sheet in geschieberite viewed along a, with proposed hydrogen bonds within the sheet.

tetrahedra, such that each bipyramid and each tetrahedron is four-connected within the sheet (Fig. 4). The free vertex of the uranyl pentagonal bipyramid, which is not involved in the linkage between pentagonal bipyramids and sulfate tetrahedra, is occupied by an H_2O molecule. The corresponding H bonds extend the inter-sheet linkage (Fig. 4). The sheets are stacked perpendicular to **a** (Fig. 3*a*). The two K atoms are localized in the interlayer between the sheets along with the remaining H_2O group. The [7]-coordinate *K*1 site and the [6]-coordinate *K*2 site serve to link adjacent sheets (Fig. 3*a*). The lack of a centre of symmetry is driven by misorientation of the SO_4 tetrahedra of the adjacent layers (Fig. 3*b*) (Alekseev *et al.*, 2006). The structural formula of geschieberite, obtained from the refinement and bond-valence analysis (Table 4), is $K_2[(UO_2)(SO_4)_2(H_2O)](H_2O)$, $Z = 4$.

Topological relations

Structural units of the same composition, $[(UO_2)(SO_4)_2(H_2O)]^{2-}$, as are present in geschieberite and in its synthetic analogue, were found by Ling *et al.* (2010) in the synthetic compound with the same structural formula, $K_2[(UO_2)(SO_4)_2(H_2O)](H_2O)$ (but with $Z = 8$). However, this compound crystallizes in space group *Cmca*, and the structural units are infinite chains of polyhedra, rather than sheets. This is the result of the depolymerizing action of H_2O groups located at the vertex of the uranyl pentagonal bipyramid that alternate along the chain.

The structural sheet present in geschieberite is topologically related to those occurring in the minerals leydetite, $Fe(UO_2)(SO_4)_2(H_2O)_{11}$ (Plášil *et al.*, 2013*a*) and wetherillite, $Na_2Mg(UO_2)_2(SO_4)_4{\cdot}18H_2O$ (IMA 2014-044).

Acknowledgements

The authors are grateful to Ladislav Lapčák (Institute of Chemical Technology, Prague) for help with Raman spectroscopic analysis. They thank Anthony Kampf for improving the English in the manuscript and for further suggestions. An anonymous reviewer and Peter Leverett are thanked for suggestions and comments that helped in improving the text. This research was financially supported as post-doctoral project 13-31276P of the Grant Agency of the Czech Republic to JP and the long-term project of the Ministry of Culture of the Czech Republic 2014/02 (National Museum, 00023272) to JČ.

References

Alekseev, E.V., Sulemanov, E.V., Chuprunov, E.V., Marychev, M.O., Ivanov, V.A. and Fukin, G.K.

https://doi.org/10.1180/minmag.2015.079.1.16 Published online by Cambridge University Press

(2006) Crystal structure and nonlinear optical properties of the $K_2UO_2(SO_4)_2.2H_2O$ compound at 293K. *Crystallography Reports*, **51**, 29–33.

Bartlett, J.R. and Cooney, R.P. (1989) On the determination of uranium-oxygen bond lengths in dioxouranium(VI) compounds by Raman spectroscopy. *Journal of Molecular Structure*, **193**, 295–300.

Brown, I.D. (1981) The bond-valence method: an empirical approach to chemical structure and bonding. Pp. 1–30 in: *Structure and Bonding in Crystals II* (M. O'Keeffe and A. Navrotsky, editors). Academic Press, New York.

Brown, I.D. (2002) *The Chemical Bond in Inorganic Chemistry: The Bond Valence Model*. Oxford University Press, Oxford, UK.

Brown, I.D. and Altermatt, D. (1985) Bond-valence parameters obtained from a systematic analysis of the inorganic crystal structure database. *Acta Crystallographica*, **B41**, 244–247, with updated parameters from http://www.ccp14.ac.uk/ccp/web-mirrors/i_d_brown/.

Burns, P.C. (2001) A new uranyl sulfate chain in the structure of uranopilite. *The Canadian Mineralogist*, **39**, 1139–1146.

Burns, P.C. (2005) U^{6+} minerals and inorganic compounds: insights into an expanded structural hierarchy of crystal structures. *The Canadian Mineralogist*, **43**, 1839–1894.

Burns, P.C., Ewing, R.C. and Hawthorne, F.C. (1997) The crystal chemistry of hexavalent uranium: polyhedron geometries, bond-valence parameters, and polymerization of polyhedra. *The Canadian Mineralogist*, **35**, 1551–1570.

Čejka, J. (1999) Infrared and thermal analysis of the uranyl minerals. Pp. 521–622 in: *Uranium: Mineralogy, Geochemistry, and the Environment* (P.C. Burns and R. Finch, editors). Reviews in Mineralogy, **38**. Mineralogical Society of America, Washington, DC.

Čejka, J. (2004) Vibrational spectroscopy of uranyl mineral – infrared and Raman spectra of uranyl minerals. I. Uranyl. *Bulletin mineralogicko-petrologického oddělení Národního muzea (Praha)*, **12**, 44–51.

Čejka, J. (2007) Vibrational spectroscopy of uranyl minerals – infrared and Raman spectra of uranyl minerals. III. Uranyl sulfates. *Bulletin mineralogicko/petrologického oddělení Národního muzea (Praha)*, **14–15**, 40–46.

Edwards, K.J., Bond, P.L., Druschel, G.K., McGuire, M.M., Hamers, R.J. and Banfield, J.F. (2000) Geochemical and biological aspects of sulfide mineral dissolution: lessons from Iron Mountain, California. *Chemical Geology*, **169**, 383–397.

Evangelou, V.P. and Zhang, Y.L. (1995) A review – pyrite oxidation mechanisms and acid mine drainage prevention. *Critical Reviews in Environmental Sciences and Technology*, **25**, 141–199.

Frondel, C., Ito, J., Honea, R.M. and Weeks, A.M. (1976) Mineralogy of the zippeite-group. *The Canadian Mineralogist*, **14**, 429–436.

Jambor, J.L., Nordstrom, D.K. and Alpers, C.N. (2000) Metal–sulfate salts from sulfide mineral oxidation. Pp. 303–350 in: *Sulfate Minerals: Crystallography, Geochemistry, and Environmental* (C.N. Alpers, J.L. Jambor and D.K. Nordstrom, editors). Reviews in Mineralogy & Geochemistry, **40**. Mineralogical Society of America and the Geochemical Society, Washington, DC.

Kampf, A.R., Plášil, J., Kasatkin, A.V. and Marty, J. (2014) Belakovskiite, $Na_7(UO_2)(SO_4)_4(SO_3OH)(H_2O)_3$, a new uranyl sulfate mineral from the Blue Lizard mine, San Juan County, Utah, USA. *Mineralogical Magazine*, **78**, 639–649.

Kraus, W. and Nolze, G. (1996) POWDER CELL – a program for the representation and manipulation of crystal structures and calculation of the resulting X-ray powder patterns. *Journal of Applied Crystallography*, **29**, 301–303.

Krivovichev, S.V. (2010) Actinyl compounds with hexavalent elements (S, Cr, Se, Mo): structural diversity, nanoscale chemistry, and cellular automata modelling. *European Journal of Inorganic Chemistry*, **2010**, 2594–2603.

Laugier, J. and Bochu, B. (2004) *LMPG Suite of Programs for the Interpretation of X-ray Experiments*. ENSP/Laboratoire des Matériaux et du Génie Physique, BP 46. 38042 Saint Martin d'Hères, France. URL: http://www.ccp14.ac.uk/tutorial/lmgp/ (Accessed: 16 January 2014).

Libowitzky, E. (1999) Correlation of O-H stretching frequencies and O-H···O hydrogen bond lengths in minerals. *Monatshefte für Chemie*, **130**, 1047–1059.

Ling, J., Sigmon, G.E., Ward, M., Roback, N. and Burns, P.C. (2010) Syntheses, structures, and IR spectroscopic characterization of new uranyl sulfate/selenate 1D-chain, 2D-sheet and 3D framework. *Zeitschrift für Kristallographie*, **225**, 230–239.

Mandarino, J.A. (1981) The Gladstone-Dale relationship: Part IV. The compatibility concept and its application. *The Canadian Mineralogist*, **19**, 441–450.

Nakamoto, K. (1986) *Infrared and Raman Spectra of Inorganic and Coordination Compounds*. John Wiley and Sons, New York.

Niinistö, L., Toivonen, J. and Valkonen, J. (1978) Uranyl(VI) compounds. I. The crystal structure of ammonium sulfate dihydrate, $(NH_4)UO_2(SO_4)_2.2H_2O$, *Acta Chemica Scandinavica*, **A32**, 647–651.

Niinistö, L., Toivonen, J. and Valkonen, J. (1979)

https://doi.org/10.1180/minmag.2015.079.1.16 Published online by Cambridge University Press

Uranyl(VI) compounds. II. The crystal structure of potassium uranyl sulphate dehydrate $K_2UO_2(SO_4)_2{\cdot}2H_2O$. *Acta Chemica Scandinavica*, **A33**, 621–624.

Oszlányi, G. and Süto, A. (2004) *Ab-initio* structure solution by charge flipping. *Acta Crystallographica*, **A60**, 134–141.

Oszlányi, G. and Süto, A. (2008) The charge flipping algorithm. *Acta Crystallographica*, **A64**, 123–134.

Palatinus, L. (2013) The charge-flipping algorithm in crystallography. *Acta Crystallographica*, **B69**, 1–16.

Palatinus, L. and Chapuis, G. (2007) Superflip – a computer program for the solution of crystal structures by charge flipping in arbitrary dimensions. *Journal of Applied Crystallography*, **40**, 451–456.

Palatinus, L. and van der Lee, A. (2008) Symmetry determination following structure solution in *P*1. *Journal of Applied Crystallography*, **41**, 975–984.

Pekov, I.V., Krivovichev, S.V., Yapaskurt, V.O., Chukanov, N.V. and Belakovskyi, D.I. (2014) Beshtauite, $(NH_4)_2(UO_2)(SO_4)_2{\cdot}2H_2O$, a new mineral from Mount Beshtau, Northern Caucasus, Russia. *American Mineralogist*, **99**, 1783–1787.

Petříček, V., Dušek, M. and Palatinus, L. (2006) *Jana2006. The Crystallographic Computing System*. Institute of Physics, Prague, Czech Republic.

Petříček, V., Dušek, M. and Palatinus, L. (2014) Crystallographic computing system JANA2006: general features. *Zeitschrift für Kristallographie*, **229**, 345–352.

Plášil, J. (2014) Oxidation–hydration weathering of uraninite: the current state-of-knowledge. *Journal of Geosciences*, **59**, 99–114.

Plášil, J., Buixaderas, E., Čejka, J., Jehlička, J. and Novák, M. (2010) Raman spectroscopic study of the uranyl sulphate mineral zippeite: low wavenumber and U–O stretching regions. *Analytical and Bioanalytical Chemistry*, **397**, 2703–2715.

Plášil, J., Dušek, M., Novák, M., Čejka, J., Císařová, I. and Škoda, R. (2011) Sejkoraite-(Y), a new member of the zippeite group containing trivalent cations from Jáchymov (St. Joachimsthal), Czech Republic: description and crystal structure refinement. *American Mineralogist*, **96**, 983–991.

Plášil, J., Hloušek, J., Veselovský, F., Fejfarová, K., Dušek, M., Škoda, R., Novák, M., Čejka, J., Sejkora, J. and Ondruš, P. (2012) Adolfpateraite, $K(UO_2)(SO_4)(OH)(H_2O)$, a new uranyl sulfate mineral from Jáchymov, Czech Republic. *American Mineralogist*, **97**, 447–454.

Plášil, J., Kasatkin, A.V., Škoda, R., Novák, M., Kallistová, A., Dušek, M., Skála, R., Fejfarová, K., Čejka, J., Meisser, N., Goethals, H., Machovič, V. and Lapčák, L. (2013*a*) Leydetite, $Fe(UO_2)(SO_4)_2(H_2O)_{11}$, a new uranyl sulfate mineral from Mas d'Alary, Lodève, France. *Mineralogical Magazine*, **77**, 429–441.

Plášil, J., Kampf, A.R., Kasatkin, A.V., Marty, J., Škoda, R., Silva, S. and Čejka, J. (2013*b*) Meisserite, $Na_5(UO_2)(SO_4)_3(SO_3OH)(H_2O)$, a new uranyl sulfate mineral from the Blue Lizard mine, San Juan County, Utah, USA. *Mineralogical Magazine*, **77**, 2975–2988.

Plášil, J., Veselovský, F., Hloušek, J., Škoda, R., Novák, M., Sejkora, J., Čejka, J., Škácha, P. and Kasatkin, A.V (2014*a*) Mathesiusite, $K_5(UO_2)_4(SO_4)_4(VO_5)(H_2O)_4$, a new uranyl vanadate-sulfate from Jáchymov, Czech Republic. *American Mineralogist*, **99**, 625–632.

Plášil, J., Kampf, A.R., Kasatkin, A.V. and Marty, J. (2014*b*) Bluelizardite, $Na_7(UO_2)(SO_4)_4Cl(H_2O)_2$, a new uranyl sulfate mineral from the Blue Lizard mine, San Juan County, Utah, USA. *Journal of Geosciences*, **59**, 145–158.

Plášil, J., Hloušek, J., Kasatkin, A.V., Škoda, R., Novák, M. and Čejka, J. (2014*c*) Geschieberite, IMA 2014-006. CNMNC Newsletter No. 20, June 2014, page 555; *Mineralogical Magazine*, **78**, 549–558.

Plášil, J., Hloušek, J., Kasatkin, A.V., Novák, M. and Čejka, J. and Lapčák, L. (2015) Svornostite, $K_2Mg[(UO_2)(SO_4)_2]_2{\cdot}8H_2O$, a new uranyl sulfate mineral from Jáchymov, Czech Republic. *Journal of Geosciences*, **60**, 113–121.

Pouchou, J.L. and Pichoir, F. (1985) 'PAP' (φ ρZ) procedure for improved quantitative microanalysis. Pp. 104–106 in: *Microbeam Analysis* (J.T. Armstrong, editor). San Francisco Press, San Francisco, California, USA.

https://doi.org/10.1180/minmag.2015.079.1.16 Published online by Cambridge University Press